

ORIGINAL ARTICLE

Erwin · Shuhei Takemoto · Won-Joung Hwang  
Miyuki Takeuchi · Takao Itoh · Yuji Imamura

## Anatomical characterization of decayed wood in standing light red meranti and identification of the fungi isolated from the decayed area

Received: July 20, 2007 / Accepted: January 16, 2008 / Published online: March 13, 2008

**Abstract** To further our understanding of wood decay in living light red meranti (*Shorea smithiana*) trees, microscopic characteristics of the cell and cell wall degradations of *S. smithiana* wood in the presence of the decay fungi, the identity of the causal fungi, and the decay potential and pattern by an isolated fungus were investigated. Cell wall degradations, including cell wall thinning, bore holes formation, rounded pit erosion, and eroded channel opening were clearly observed under light and scanning electron microscopy. In transverse view, many large voids resulting from a coalition of degraded wood tissue appeared in the decayed canker zone. All these observations suggest the well-known simultaneous decay pattern caused by white-rot fungi. By phylogenetic analysis based on the sequences of internal transcribed spacer region of ribosomal DNA, a basidiomycete fungus isolated from the decayed wood was identified as *Schizophyllum commune*. The degradation caused by this fungus on sound *S. smithiana* wood in an in situ laboratory decay test was classified as the early stage of simultaneous decay, and showed a similar pattern to that observed in the wood samples naturally decayed.

**Key words** *Shorea smithiana* · Wood decay · White-rot fungus · Phylogenetic analysis

### Introduction

Because the decay of wood of living trees is a long-standing problem, the degradation of wood caused by decay fungi has been well characterized.<sup>1</sup> Nevertheless, such studies must continue because wood decay has not yet been investigated in many types of trees. One such example is basal stem canker of light red meranti (*Shorea smithiana* Sym.), a dipterocarp found growing naturally in Bukit Soeharto Forest in East Kalimantan, Indonesia.

*Shorea smithiana*, which grows in the lowlands of the Southeast Asian tropical rainforest, is a member of the Dipterocarpaceae family. Its timber is known as a member of the light red meranti group of timbers. The timber has been used in the manufacture of plywood, fiberboard, particleboard, molding, and other building materials. These species have also been established in large-scale plantation forests. Because such forests are managed for timber production, decay that develops on the tree stems reduces grade quality or timber yield, and is therefore a serious economic problem.

Studying the microscopic characteristics of wood degradation and identifying the fungi involved in decay of the living tree of this commercial species will help to develop control measures against decay. Identifying the causal fungi and examining the decay pattern on wood caused by these isolated fungi in the laboratory should enable confirmation of the cause of degradation of the living wood.

The present study aimed to (1) elucidate the microscopic features of naturally decayed wood in a *S. smithiana* tree using light and scanning electron microscopy; (2) identify the decay fungi isolated from the decayed tissue based on the sequences of the internal transcribed spacer (ITS) region of ribosomal DNA (rDNA); and (3) evaluate the decay potential and decay pattern of the decay fungi on *S. smithiana* wood in laboratory studies.

Erwin (✉) · M. Takeuchi · T. Itoh · Y. Imamura  
Research Institute for Sustainable Humanosphere, Kyoto University,  
Gokasho, Uji, Kyoto 611-0011, Japan  
Tel. +81-774-38-3663; Fax +81-774-38-3664  
e-mail: erwin@rish.kyoto-u.ac.jp

S. Takemoto  
Plant Pathology Research Team, National Institute of Fruit Tree  
Science, National Agriculture and Food Research Organization,  
Tsukuba, Ibaraki 305-8605, Japan

W.-J. Hwang  
Institute of Wood Technology, Akita Prefectural University,  
Noshiro, Akita 016-0876, Japan

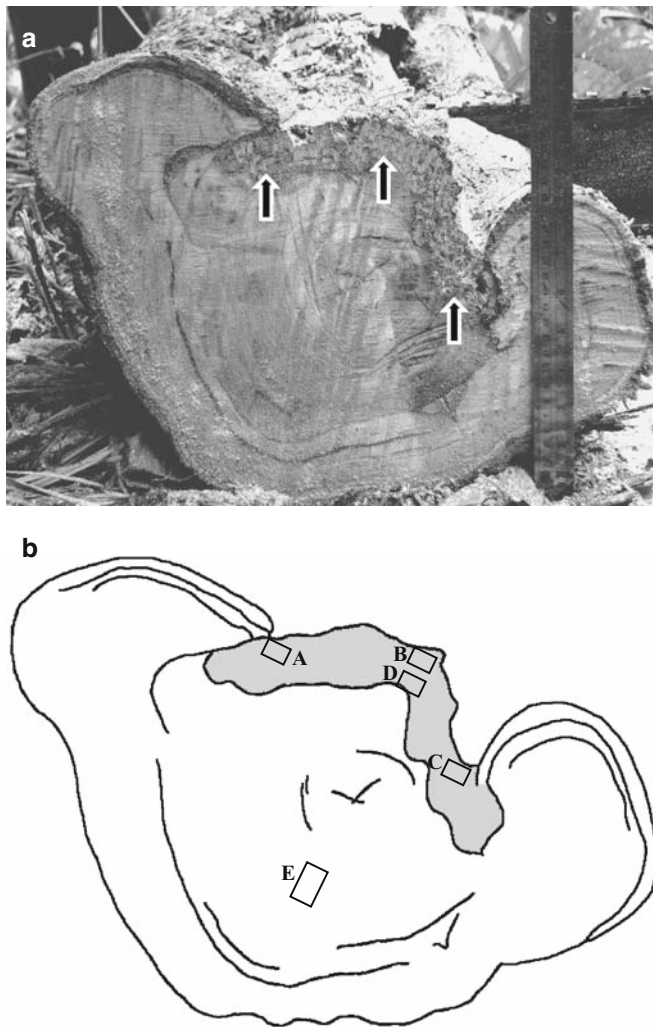


**Fig. 1.** **a** Cross-cut surface of *Shorea smithiana* log with exposed wood showing decay at the canker margin (arrows). **b** Sketch of **a** describing the zoning of the cut surface and the sites of sample collection. Decayed zone is shaded gray: A–C, decayed wood in the canker margin; D, decayed wood adjacent to the region of sound wood; E, sound wood opposite the region of decayed wood

## Materials and methods

### Wood sample collections

Wood samples were collected from a 45-year-old specimen of *Shorea smithiana* cankerous tree [diameter at breast height (DBH) approximately 55 cm] growing in a natural dipterocarp stand at the Bukit Soeharto Educational Forest of Mulawarman University, East Kalimantan, Indonesia. It was one of the typical trees diseased with canker, and such trees were frequently found in the *S. smithiana* stand in that region. The canker with decayed wood was formed on the stem from ground level up to 50 cm (Fig. 1). Four disks 5 cm thick were cut from the decayed stem. Three of these disks were used for microscopic observations of the anatomical characteristics of wood decay, and a fourth disk was used to isolate decay fungi. The sound, healthy portions were cut

out from these disks and used for an in vitro laboratory decay test.

### Isolation of wood-decaying fungi

The medium used for isolating wood-decaying fungi was 2% malt extract agar (pH 5.5) (MEA, 20 g of malt extract and 15 g of Difco agar in 1000 ml distilled water) with 100 ppm of chloramphenicol (antibiotic), and 2% MEA with 100 ppm of chloramphenicol and 100 ppm of benomyl (a fungicide with broad-spectrum activity on ascomycetes). All media were sterilized by autoclaving at 0.103 MPa at 121°C for 20 min.

Three small pieces of wood (approximately 5 × 5 × 5 mm) were cut from decayed and sound sites on the disk (Fig. 1b): decayed wood in the canker margin (A–C), decayed wood adjacent to the region of sound wood (D), and sound wood away from the region of decayed wood (E). All wood samples were aseptically transferred to culture media in petri dishes and then incubated at room temperature (24°C) for several days. A small piece of agar containing fungal mycelium was transferred separately from the margin of the colony growing from each of the wood samples onto 2% MEA containing 100 ppm of chloramphenicol plated in a petri dish to purify the cultures. The medium was amended with 100 ppm of benomyl to obtain selective growth of basidiomycete fungi. Finally, 30 isolates were established. Each fungal isolate was categorized into morphotype based on its colony appearance, growth pattern, and spore morphology, if available. One isolate arbitrarily selected from each morphotype was later transferred to 5 ml of liquid medium (20 g of malt extract in 1000 ml of distilled water) in test tubes and incubated at room temperature for 3–5 days. Prior to transferring the fungal isolate, the liquid medium was sterilized as previously described. The young mycelium was used for fungi identification based on the ITS sequence.

### Microscopic observations

From each of the decayed stem disks, a wood sample (approximately 15 × 15 × 15 mm) was taken from each of the five sites as mentioned above for fungi isolation (Fig. 1b). All wood samples were fixed in 2.5% glutaraldehyde, post-fixed in osmium tetroxide, dehydrated in 50%, 70%, and 95% ethanol, each for 20 min, then three times in 100% ethanol, and embedded in Epon 812 resin. Transverse, radial, and tangential sections 20–50 mm thick were cut using a diamond knife, double-stained with safranin-fast green, and examined under a light microscope. For scanning electron microscopy, each of the wood samples was fixed in 2.5% glutaraldehyde in 0.1 M phosphate buffer (pH 7.2) at 4°C overnight, washed four times in 0.1 M phosphate buffer at pH 7.2 for 15 min each, and rinsed three times in distilled water for 5 min each. The samples were dehydrated in 50%, 70%, and 95% ethanol, each for 20 min, then three times in 100% ethanol. The dehydrated samples were

freeze-dried, mounted on stubs, and then coated with gold–palladium prior to examination with a Jeol Scanning Microscope (JSM-5310).

#### DNA extraction and purification from fungal mycelia

Fungal mycelium (corresponding to ca. 2 mg after drying) was transferred directly from liquid culture using a sterile inoculation wand into a microtube for DNA extraction. DNA extraction and polymerase chain reaction (PCR) conditions generally followed the method described by Matsuda and Hijii,<sup>2</sup> which was modified from that of Gardes and Bruns.<sup>3</sup> The fungal mycelia were rinsed twice with CTAB buffer [50 mM Tris-HCl pH 8.0, 0.7 M NaCl, 10 mM ethylenediaminetetraacetic acid (EDTA), 1% cetyltrimethylammonium bromide, 0.5% poly(vinyl pyrrolidone)]. CTAB lysis buffer (200  $\mu$ l) was added to microtubes containing fungal mycelium and the tubes were subjected to three thaw cycles (from liquid nitrogen to hot water bath at 65°C). After the final thaw, the tissues were ground with a micropestle and incubated at 65°C for 45–60 min. Chloroform–isoamyl alcohol (200  $\mu$ l; 24:1) was added to microtubes containing the incubated tissue and centrifuged (15 000 g) at 4°C for 20 min. After the supernatants were transferred to other microtubes, the DNA was precipitated by the addition of 200  $\mu$ l of cold isopropanol and then by centrifugation. The DNA pellet was washed with 1 ml of 70% ice-cooled ethanol by centrifugation, then dried and resuspended in 60  $\mu$ l TE buffer (10 mM Tris-HCl, 1 mM EDTA, pH 8.0).

#### PCR amplification

The ITS and 5.8S gene of rDNA of fungal isolates were amplified using PCR with total reaction volume of 25  $\mu$ l (template DNA, ca. 0.5 ng/ $\mu$ l; each dNTPs, 200  $\mu$ M; Taq DNA polymerase (New England Biolabs), 0.5 U; each primer, 0.5  $\mu$ M, Tris-HCl, 1 mM; KCl, 5 mM). The PCR mixture was prepared according to the manufacturer's instruction. A primer set, ITS 1F (5'-CTT GGT CAT TTA GAG GAA GTA A-3') and ITS 4 (5'-TCC TCC GCT TAT TGA TAT GC-3'), designed by White et al.,<sup>4</sup> was used; however, when the PCR was unsuccessful, the forward primer ITS1F was replaced by an alternative primer, ITS5 (5'-GGA AGT AAA AGT CGT AAC AAG G-3') also designed by White et al.<sup>4</sup> The cycling condition and PCR temperature were adjusted following the method of Gardes and Bruns.<sup>3</sup> For checking DNA contamination of the reaction mixtures, negative controls (no DNA templates) were used. The amplified PCR products were then separated in 0.7% agarose gels and visualized using ethidium bromide. The PCR products were recovered from the gels and were manually purified as previously described.

#### DNA sequencing and analysis

The purified PCR products were sequenced according to the method described by White et al.<sup>4</sup> for the ITS1, ITS2,

and 5.8S regions of nuclear ribosomal DNA, using the primers ITS1F, ITS5, and ITS4. DNA sequences were determined using an ABI Prism 310 Genetic Analyzer (Applied Biosystems, CA, USA). The DNA sequence determined for each fungus was aligned together with that of known species in the GenBank database [National Centre for Biotechnology Information (NCBI) US National Institute of Health Bethesda (<http://www.ncbi.nlm.nih.gov/>)]. The computer software "GENETYX-MAC Ver.11.2" was used for the alignment. Identification at the genus level was based on identities above 95% following the method of Landeweert et al.<sup>5</sup> For basidiomycetes, further analysis was conducted using Clustal W version 1.83<sup>6</sup> via the online analysis service of the DDBJ (<http://clustalw.ddbj.nig.ac.jp/top-e.html>). A default set of the parameters was used for the alignment and phylogenetic analysis. Phylogenetic relationships were inferred using the "Bootstrap N-J" (neighbor-joining) tree<sup>7</sup> program in Clustal W based on Kimura-2-parameter distance. To evaluate the strength of support for the branches of the N-J trees, 1000 replications of bootstrap analysis were performed. The tree was displayed using TreeView PPC 1.6.6.<sup>8</sup>

#### Decay test

Twelve sound wood blocks (20  $\times$  20 mm in cross section  $\times$  10 mm in length) obtained from the uninfected portions of the stem disks (site E in Fig. 1b) were inoculated with the isolated fungus, and incubated in accordance with the JIS K 1571 soil-block test procedure.<sup>9</sup> The wood blocks were sterilized with gaseous ethylene oxide at 50°C for 5 h after oven drying and weighing. Three blocks were placed in each one of four glass jars containing a medium of 250 g quartz sand and 80–85 ml of nutrient solution (4.0% glucose, 0.3% peptone, and 1.5% malt extract) and inoculated with the liquid fungal culture of the isolated fungus. The four glass jars were then incubated at 26  $\pm$  2°C and 70%–80% relative humidity for 12 weeks. In order to verify weight loss, nine blocks were oven-dried at 70°C until a constant dry weight was obtained; three blocks were reserved for anatomical observations.

## Results

#### Microscopic evidence of *Shorea smithiana* decayed wood in the forest

A transverse view of the stem canker of *Shorea smithiana* shows what appears to be decay in the exposed wood at the canker margin. The decay appeared to extend from outside to inside and also tangentially (Fig. 1a, b). Examination by light and scanning electron microscopy on the decayed wood showed that various stages of simultaneous decay could be observed (Figs. 2–8). Schwarze et al.<sup>1</sup> noted that at the early stage of simultaneous wood decay, cell-wall degradation occurred in the immediate vicinity of the hyphae, and the cell wall was progressively broken down

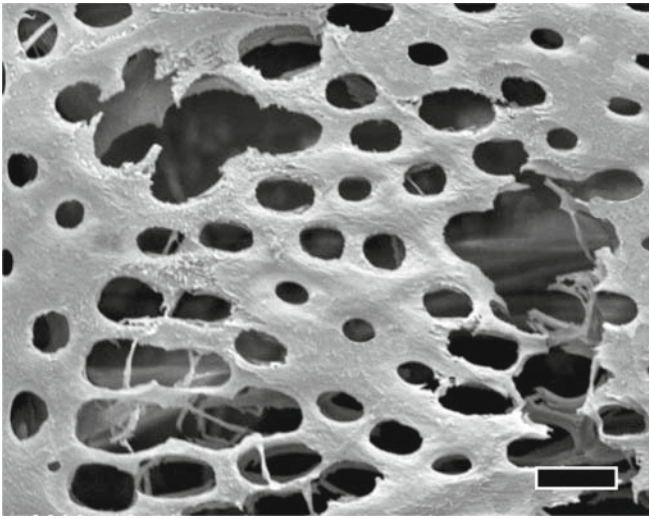


**Fig. 2.** Rounded erosion of intervessel pits, followed by the coalescence of the rounded pits. The sample was prepared from site *D* shown in Fig 1b. Bar 10  $\mu\text{m}$

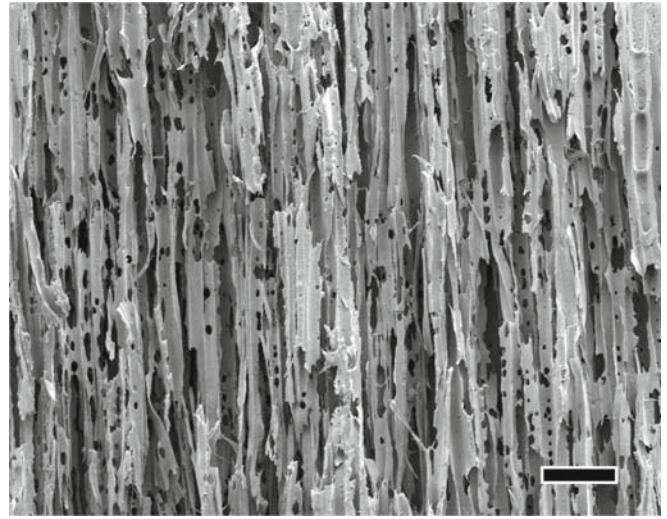


**Fig. 4.** Erosion troughs and numerous conspicuous holes were evident within fiber and parenchymal cell walls. The sample was prepared from site *A* shown in Fig 1b. Bar 100  $\mu\text{m}$

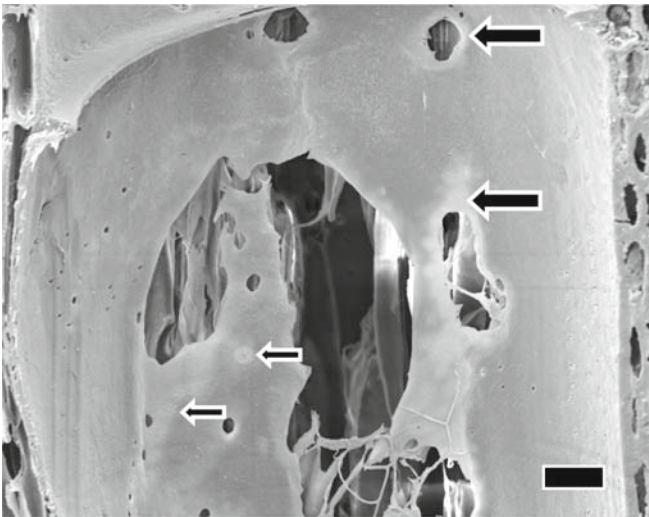


**Fig. 3.** Enlarged bore holes and axially elongated erosion troughs appeared in vessel walls. Lysis zones appeared around the bore holes and the erosion trough (large arrows), and as round spots (small arrows). The sample was prepared from site *D* shown in Fig 1b. Bar 20  $\mu\text{m}$



**Fig. 5.** Erosion channels with U-notches in fiber cell wall (arrow). The sample was prepared from site *A* shown in Fig 1b. Bar 20  $\mu\text{m}$

from the inside (cell lumen) to the outside; at the intermediate stage the cell wall became increasingly thinner, and numerous bore holes appeared between two neighboring cells. At the late decay stage, the compound of middle lamella and cell corner degraded.

At the early stage of decay of wood cells, we observed basidiomycete hyphae colonizing the cell lumina and passing through cells via pit apertures with rounded pit erosion, bore hole formation in unpitted cell walls, and slight erosion of cell walls (Fig. 2). In vessel cell walls, as shown in Fig. 2, destruction of the intervessel pits occurred, appearing as rounded and distorted openings. Sometimes the intervessel walls were severely damaged. Figure 3 shows enlarged and

coalesced bore holes, which then continued to be eroded until axially elongated troughs were formed.

At the intermediate decay stage, numerous and conspicuous holes with irregular rims were observed in fiber and axial parenchyma cell walls (Fig. 4). Fiber degradation was frequently observed in regions where ray parenchyma cells were in contact with degraded fibers (Fig. 5). Cell thinning could also be observed in some fiber and axial parenchyma cells, which resulted in wood cells becoming deformed (Fig. 6).

In transverse sections, the late decay stage was clearly detected, as shown in Fig. 6. Partial degradation of the cell wall had a channel-like appearance in some fiber and axial parenchyma cells, which were connected to neighboring cells. With increasing decay, these channels enlarged and

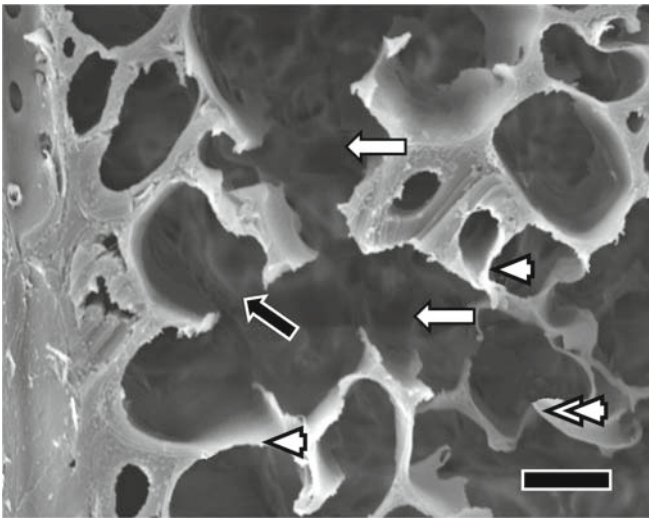


**Fig. 6.** Thinning (single-head arrows) and collapse (double-head arrow) of the cell walls, erosion channel (black arrow), and complete removal of cells (white arrows), which simultaneously occurred in one region of decay. The sample was prepared from site C shown in Fig 1b. Bar 10  $\mu\text{m}$

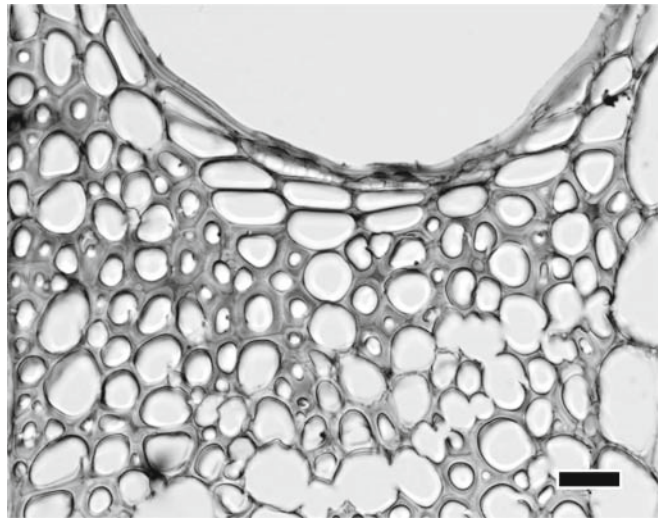


**Fig. 8.** Lignin remained in the cell corners and middle lamella, which were stained red by double staining with safranin-fast green at a progressive stage of decay. The sample was prepared from site D shown in Fig 1b. Bar 20  $\mu\text{m}$

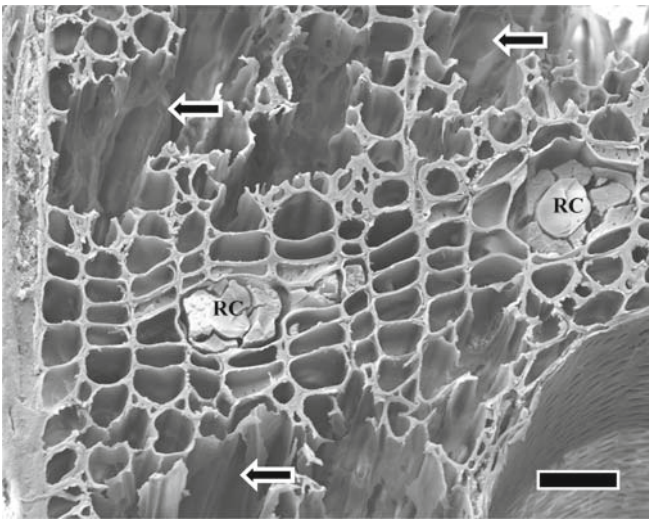


**Fig. 7.** Axial parenchyma cells adjacent to resin canals (RC) remained relatively unaltered. Note large voids (arrows) resulting from complete degradation of cell wall components within the degraded area. The sample was prepared from site B shown in Fig 1b. Bar 40  $\mu\text{m}$

joined to form cavities, decaying whole parts of the cell walls and also the middle lamella and cell corners. Due to the complete removal of all cell components, the remaining wood cells appeared to be separate from each other. Complete degradation of cell wall components resulted in many large voids that appeared in transverse sections of the decayed wood, as shown in Fig. 7. Advanced wood decay was also clearly observed in the severely degraded paratracheal parenchyma cells, while only axial parenchyma cells adjacent to resin canals remained (Fig. 7).

After double staining with safranin fast-green, light microscopy revealed that the middle lamella and cell corners with residual lignin were stained red, whereas the remaining

fiber and axial parenchyma cell walls were mainly stained green, possibly due to the abundance of cellulose and hemicellulose (Fig. 8).

#### Identification of decay fungi based on DNA sequence

Only one fungus was isolated from decayed tissue cultured on MEA with benomyl and chloramphenicol. This fungus had clamp connections on its hyphae, indicating that it was a basidiomycete. However, when 2% MEA medium with chloramphenicol (without benomyl) was used, two species of nondecaying mitospore fungi were isolated, and no basidiomycete was detected.

When compared with sequences in the GenBank database, the ITS sequence of the basidiomycete isolate and the nondecaying fungi had more than 99% homology with the sequences of their closest matching species (Table 1). To complement the results of a BLAST search, we aligned the sequences of basidiomycete decay fungus (fungus RM4ac) with downloaded sequences from the GenBank database and performed phylogenetic analysis using Clustal W (Fig. 9). The fungus RM4ac isolate resided within the clade of *Schizophyllum commune* and *Schizophyllum radiatum*, a result supported by a high bootstrap value (973/1000) in the phylogenetic tree.

#### Microscopic evidence of *Shorea smithiana* wood decayed by *Schizophyllum commune* in the laboratory

After 12 weeks of exposure in the laboratory decay test, wood blocks of *S. smithiana* that had been inoculated with *S. commune* fungus sustained an average weight loss of 1.8%. After initial colonization on the surface of *S. smithiana* wood, the hyphae of *S. commune* penetrated into the

**Table 1.** List of the fungal isolates from the decayed wood of *Shorea smithiana* stem canker and fungal species deduced from their internal transcribed spacer sequences

Code name <sup>a</sup>	Accession number <sup>b</sup>	Closest match <sup>c</sup> (accession number)	Homology <sup>d</sup> (bps)
RM3	AB297717	<i>Penicillium daleae</i> (DQ132832)	99% (510)
RM4	AB297720	<i>Trichoderma asperellum</i> (DQ109538)	100% (411)
RM4ac	AB297718	<i>Schizophyllum commune</i> (AF280758)	100% (632)

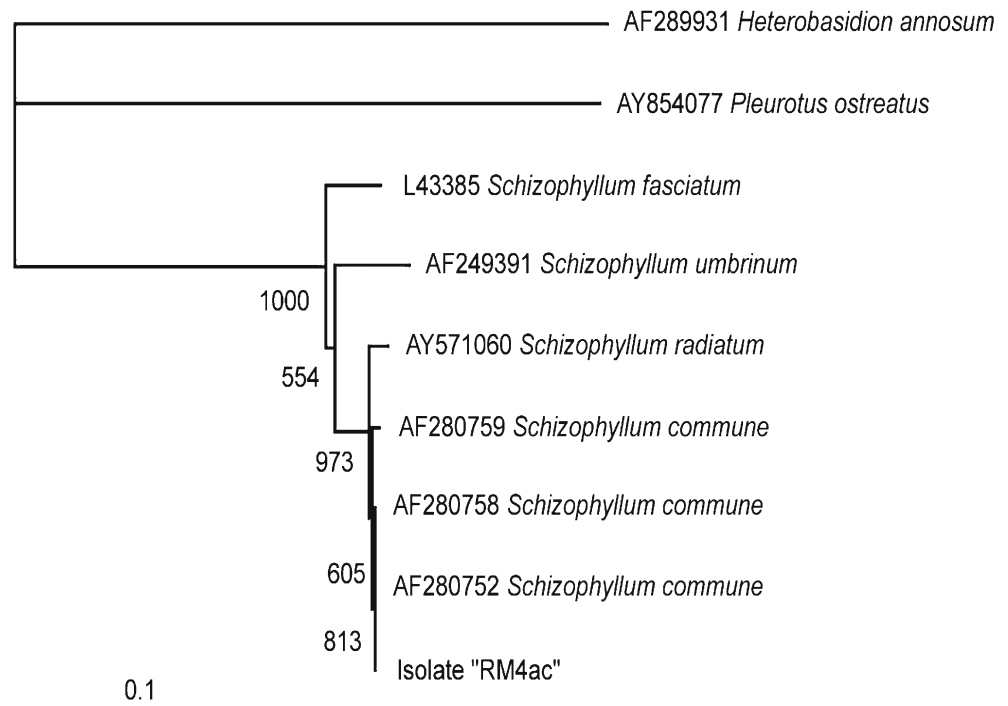
<sup>a</sup> Code names for the fungal isolates

<sup>b</sup> Accession numbers for the DNA sequences of the isolates

<sup>c</sup> The name of fungal species registered in GenBank that had a sequence with the highest homology to the DNA sequence of the isolates. Unidentified species were ignored

<sup>d</sup> The homology between reference sequences of the closest match and query sequences of the isolates. Total length of the query sequences are shown in parentheses

**Fig. 9.** Neighbor-joining tree derived from the internal transcribed spacer sequences of a fungus isolated from the decayed wood of *Shorea smithiana* stem canker and reference strains from GenBank. The tree was rooted by the outgroup using the sequence of an Aphylophorales fungus, *Heterobasidion annosum*. Bootstrap values higher than 500 out of 1000 are indicated. Bar stands for genetic distance (the number of nucleotide substitution per site)



inner tissues. Hyphae appeared in the lumen of all cell types but were abundant mainly in vessels. The spread of fungal hyphae did not appear to cause extensive degradation of wood cells, and the intensive erosion and thinning of cell walls that occurred in decayed wood of the living tree were not detected. Nevertheless, signs of decay such as erosion troughs and pit degradation were frequently detected in infected cells. It appeared that hyphal branches penetrated to the vessel wall mainly through pits that caused distortion and enlarged openings (Fig. 10). Presence of erosion troughs in fibers and hyphae passing through pits were also observed in axial parenchyma cell walls (Figs. 11 and 12).

## Discussion

The presence of decayed wood at the canker margin indicating wound or injury was initiated by infection with decay fungi on the *Shorea smithiana* tree. With very few excep-

tions (e.g., wound parasites), it was shown empirically that most decay fungi preferentially infect and colonize the injured parts of the stem in which sapwood or heartwood is exposed.<sup>1</sup>

The three major types of wood decay are white, brown, and soft rots.<sup>1,10</sup> In white-decayed wood, two decay patterns have been well recognized: (1) simultaneous erosion, in which all wood cell wall components are degraded more or less simultaneously, and (2) selective delignification, in which lignin is broken down more than hemicellulose and cellulose. On the decayed wood of the living *S. smithiana* tree, the typical features of the simultaneous removal of all wood components were readily apparent. Degrading pits of cells, bore hole formation, thinning of secondary cell walls, and extensive cell wall erosion (Figs. 2–8), which are characteristic micromorphological features of simultaneous decay, were frequently detected in the present study. Similar patterns of wood degradation have also been recognized in other decayed broad-leaved trees, for instance, in beech trees.<sup>1</sup>

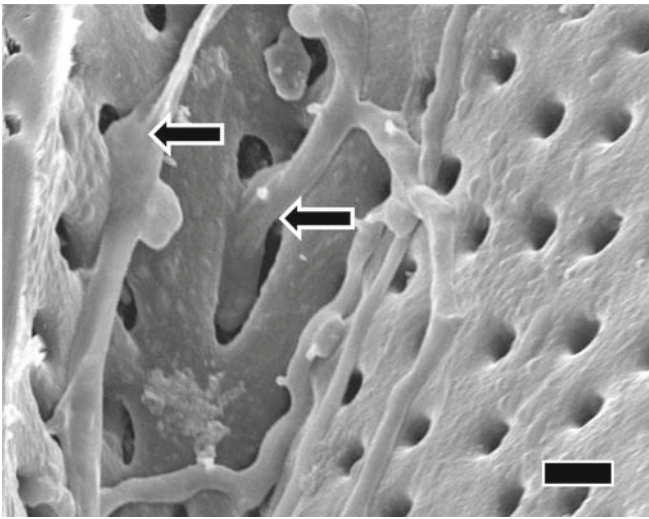


**Fig. 10.** Hyphal branches of *Schizophyllum commune* fungus passed through the vessel pits of *S. smithiana* wood after the laboratory decay test. Bar 5  $\mu$ m

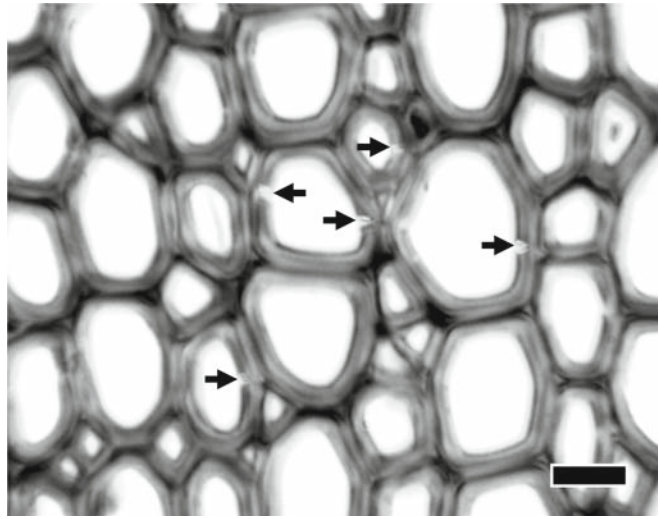


**Fig. 12.** Erosion troughs in fiber cell walls (arrows) of *S. smithiana* wood after the laboratory decay test. Bar 10  $\mu$ m

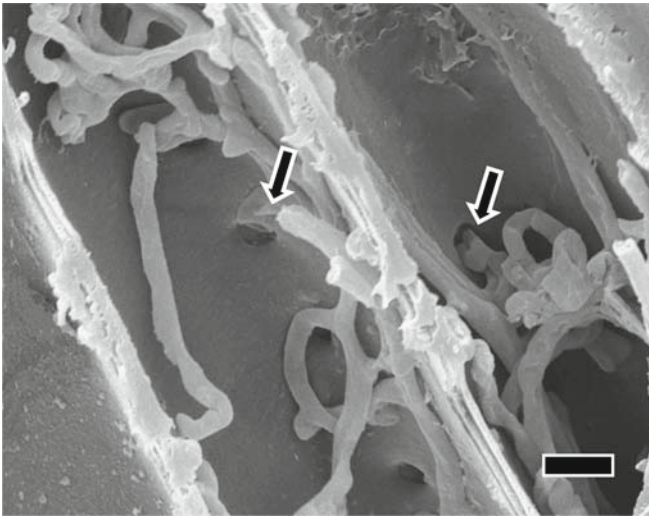


**Fig. 11.** *Schizophyllum commune* hyphae penetrated parenchyma cell walls through pits of *S. smithiana* wood after the laboratory decay test. Bar 5  $\mu$ m

The presence of numerous holes and degraded pits in cell walls (Figs. 2 and 3) indicated that hyphae passed through cells both radially and tangentially, severely degrading cell walls. The subsequent erosion of cell walls is believed to be caused by enzymatic degradation.<sup>11</sup> Fungal enzymes that attack lignin, cellulose, or hemicellulose may be too large to diffuse into sound wood<sup>12</sup> and cause extensive degradation of wood elements not in direct contact with fungal hyphae.<sup>13</sup> The lysis zones that developed around bore holes, axially elongated troughs, and pits in cells, and which also appeared as round spots (Fig. 3), clarified the effects of fungal enzymes on cell walls, which were gradually eroded. The lysis zones indicated predelignification before the formation of actual bore holes, axially elongated troughs, and

degraded pits. Liese<sup>14</sup> suggested that these simultaneous lyses of cell wall layers became progressively larger as the period of infection progressed, which might lead to large openings between cells. The erosion of the cell wall with axially elongated trough formation was also detected by Levin and Castro<sup>15</sup> in the simultaneous decay of poplar wood caused by the white-rot fungus *Trametes trogii*.

The characteristic decay pattern of cell wall thinning and channel openings were seen in the same regions of canker wood, as shown on Fig. 6, indicating that progressive decay proceeded from the secondary wall (cell lumen) toward the middle lamella. After progressive thinning of cell walls, the secondary walls were occasionally removed; only the middle lamella and cell corners remained. In channel formation, the compound middle lamella was apparently degraded and lost prior to opening. Cell degradation from the inside (lumen) to the outside has often been described as the pattern typical of simultaneous white rot.<sup>1,16</sup> Erosion channels with rounded edges (U-shaped notches) as well as enlargement of pit apertures were also readily observed in this study (Fig. 5). These typical aspects of the wood degradation were categorized by Anagnost<sup>17</sup> as simultaneous white rot associated with basidiomycete fungi.

The wood cells adjacent to axial resin canals remained intact (Fig. 7) probably because of terpenes, terpenoids, and polyisoprenes,<sup>18</sup> which are emitted from the resin canals and are toxic to decay fungi;<sup>19,20</sup> hence, those cells were locally protected from the invading fungi colonizing the vicinity of advanced decay regions.

It is interesting that only one basidiomycete species was isolated from the decayed wood tissue of *S. smithiana*. Based on the analysis shown in Fig. 9, the fungus RM4ac isolate resided within the clade of *Schizophyllum commune* and *Schizophyllum radiatum*. Furthermore, the fungus RM4ac had an ITS sequence identical to that of *S. commune* (AF280758). These results strongly suggest that RM4ac can be identified as *S. commune*. This fungal species, commonly

known as a white-rot fungus, has also been isolated from many decayed trees, for example, *Ocotea usambarensis*<sup>21</sup> and Chinese peach trees.<sup>22</sup>

The results of our laboratory decay test, in which *S. commune* induced weight loss of *S. smithiana* wood only slightly, were in accordance with previous studies that reported a weight loss of 0.5%–6.8% in various wood species after 2–7 months of incubation.<sup>23,24</sup> These findings are in agreement with the assertion of Schmidt and Liese<sup>23</sup> and Abdurachim<sup>24</sup> that this fungus is a serious wood destroyer under natural conditions, especially in tropical regions, but causes little wood decay in vitro. Laboratory conditions may not have been suitable for the fungus to extensively degrade wood despite colonization by the fungus. The degradation of wood in living trees may be due to the combined activities of many microorganisms. The presence of mold fungi such as *Penicillium* and *Trichoderma* in decayed wood could stimulate the rate of decay.<sup>25</sup>

The micromorphological changes in the cell walls of *S. smithiana* wood after 12 weeks of incubation provided important information about the pattern of the slight wood decay caused by *S. commune* under laboratory conditions. Light and scanning electron microscopy clearly revealed the hyphal penetration through the interelemental cell walls and their proliferation and colonization in the cell lumina, as well as the ability of this fungus to degrade the wood tissues.

Besides the longitudinal movement of hyphae in vessels, fibers, and axial parenchyma cells, and radial movement in ray parenchyma cells, hyphae colonized wood tissues by spreading from cell to cell via pit apertures and by penetrating across cell walls (bore holes). The degraded pits became enlarged without rupturing, suggesting that enzymes may be involved in the degradation of cell wall components around the pits. The presence of hyphae within the fiber S3 layers as well as in the erosion troughs of cell walls indicated that cell walls were progressively degraded from the cell lumen toward the middle lamella. These characteristics of wood cell degradation correspond to the simultaneous decay pattern characterized by white-rot fungi. When simultaneous decayers degrade wood tissues in vitro, erosion troughs are frequently detected in cell walls.<sup>15,17</sup> Although the erosion of wood cell walls did not appear to be extensive under laboratory conditions, light and scanning electron microscopy helped to determine that the patterns of decay in *S. smithiana* wood caused by *S. commune* were similar to those of simultaneous decay in the living *S. smithiana* tree.

*Schizophyllum commune* has not previously been reported to cause decay of *S. smithiana* trees. However, the presence of *S. commune* as a single basidiomycete fungus in the decayed wood of the *S. smithiana* tree, as well as its ability to produce in vitro a wood-decay pattern similar to that in a decayed cankerous tree, suggest that this fungus may be one of the causal agents of wood decay in *S. smithiana* trees. A further inoculation experiment is required to confirm the pathogenicity of *S. commune* to *S. smithiana*.

**Acknowledgments** The authors are grateful to Prof. Kazuyoshi Futai of the Laboratory of Environmental Mycoscience, Graduate School of Agriculture, Kyoto University, for DNA analysis of the fungi and Dr. Rina Sriwati of the same laboratory for valuable suggestions.

## References

- Schwarze FW, Engels J, Mattheck C (2000) Fungal strategies of wood decay in trees. Springer, Berlin Heidelberg New York, pp 33–138
- Matsuda Y, Hiji N (1999) Characterization and identification of *Strobilomyces confusus* Ectomycorrhizas on Momi Fir by RFLP analysis of the PCR-amplified ITS region of the rDNA. J For Res 4:145–150
- Gardes M, Bruns TD (1993) ITS primers with enhanced specificity for basidiomycetes – application to the identification of mycorrhizae and rust. Mol Ecol 2:113–118
- White TJ, Bruns T, Lee S, Taylor J (1990) Amplification and direct sequencing of fungal ribosomal RNA genes for phylogenetics. In: Innis MA, Gelfand DH, Sninsky JJ, White TJ (eds) PCR protocols. Academic, San Diego, pp 315–322
- Landeweert R, Leeflang P, Kuyper TW, Hoffland E, Rosling A (2003) Molecular identification of ectomycorrhizal mycelium in soil horizons. Appl Environ Microbiol 69:327–333
- Thompson JD, Higgins DG, Gibson TJ (1994) CLUSTAL W: improving the sensitivity of progressive multiple sequence alignment through sequence weighting, position-specific gap penalties and weight matrix choice. Nucleic Acids Res 22:4673–4680
- Saitou M, Nei M (1987) The neighbor-joining method: a new method for reconstructing phylogenetic trees. Mol Biol Evol 4:406–425
- Page RDM (2001) TreeView PPC version 1.6.6. Institute of Biomedical and Life Sciences, University of Glasgow, Glasgow
- Japanese Standards Association (2004) JIS K 1571. Test methods for determining the effectiveness of wood preservatives and their performance requirements. Japanese Standards Association, Tokyo, pp 3–10
- Schmidt O (2006) Wood and tree fungi. Biology, damage, protection, and use. Springer, Berlin Heidelberg New York, pp 135–146
- Leonowicz A, Cho NS, Luterek J, Wilkolazka A, Wasilewska MW, Matuszewska A, Hofrichter M, Wesenberg D, Rogalski J (2001) Fungal laccase: properties and activity on lignin. J Basic Microbiol 41:185–227
- Hirano T, Enoki A, Tanaka H (2000) Immunogold labeling of an extracellular substance producing hydroxyl radicals in wood degraded by brown-rot fungus *Tyromyces palustris*. J Wood Sci 46:45–51
- Takano M, Abe H, Hayashi N (2006) Extracellular peroxidase activity at the hyphal tips of the white-rot fungus *Phanerochaete crassa* WD1694. J Wood Sci 52:429–435
- Liese W (1970) Ultrastructural aspects of woody tissue disintegration. Annu Rev Phytopathol 8:231–258
- Levin L, Castro MA (1998) Anatomical study of the decay caused by the white-rot fungus *Trametes trogii* (Aphyllophorales) in wood of salix and populus. IAWA J 19:169–180
- Luna ML, Murace MA, Keil GD, Otano ME (2004) Pattern of decay caused by *Pycnoporus sanguineus* and *Ganoderma lucidum* (Aphyllophorales) in poplar wood. IAWA J 25:425–433
- Anagnost SE (1998) Light microscopic diagnosis of wood decay. IAWA J 19:141–167
- Back EL (2002) Pattern of parenchyma and canal resin composition in softwoods and hardwoods. J Wood Sci 48:167–170
- Nerg AM, Heijari J, Viitanen H, Vuorinen M, Kainulainen P, Holopainen JK (2004) Significance of wood terpenoids in the resistance of Scots pine provenances against the Old house borer, *Hylotrupes bajulus*, and brown-rot fungus, *Coniophora puteana*. J Chem Sci 30:125–141
- Matsushita YI, Hwang YH, Sugamoto K, Matsui T (2006) Antimicrobial activity of heartwood components of sugi (*Cryptomeria japonica*) against several fungi and bacteria. J Wood Sci 52: 552–556



21. Nsolomo VR, Venn K, Solheim H (2000) The ability of some fungi to cause decay in the East African camphor tree, *Ocotea usambarensis*. *Mycol Res* 104:1473–1479
22. Dai YC (2005) First report of sapwood rot of peach caused by *Schizophyllum commune* in China. *Plant Dis* 89:778
23. Schmidt O, Liese W (1980) Variability of wood degrading enzymes of *Schizophyllum commune*. *Holzforschung* 34:67–72
24. Abdurachim MRA (1965) Laboratory test with *Schizophyllum commune* Fr. *Rimba Indonesia* 10:34–46
25. Blanchette RA, Shaw CG (1978) Association among bacteria, yeasts, and basidiomycetes during wood decay. *Phytopathology* 68:631–637